

Orientation phase transition in Fe_3BO_6 : Experimental determination of the order of the transition

L. T. Tsymbal,^{1,*} Ya. B. Bazaliy,^{1,2} L. N. Bezmaternykh,³ A. Slawska-Waniewska,⁴ S. V. Vasiliev,¹ N. Nedelko,⁴
A. I. Linnik,¹ A. N. Cherkasov,¹ Yu. I. Nepochatykh,¹ V. Yu. Dmitrenko,¹ G. N. Kakazei,⁵ and P. E. Wigen⁶

¹*O. Galkin Donetsk Physics and Technology Institute, National Academy of Science of Ukraine, Donetsk, Ukraine*

²*IBM Almaden Research Center, San Jose, California 95120, USA*

³*Kirensky Institute of Physics, Krasnoyarsk, Russia*

⁴*Institute of Physics, Polish Academy of Science, Warsaw, Poland*

⁵*Institute of Magnetism, National Academy of Science of Ukraine, Kyiv, Ukraine*

⁶*Department of Physics, Ohio State University, Columbus, Ohio 43210, USA*

(Received 18 July 2006; published 30 October 2006)

Magnetization, coercive force, radio frequency, and static susceptibilities were measured near the magnetic orientation phase transition point of the Fe_3BO_6 crystal. The data exhibit characteristic features of both first and second order transitions, thus indicating the nearly intermediate nature of the Γ_2 - Γ_4 transition in this material.

DOI: [10.1103/PhysRevB.74.134429](https://doi.org/10.1103/PhysRevB.74.134429)

PACS number(s): 75.30.Kz, 75.30.Cr, 75.50.Ee

I. INTRODUCTION

The experimental observation of ultrafast magnetic dynamics in antiferromagnets¹⁻³ renewed the interest in orientation phase transition in such materials. The Fe_3BO_6 compound is a canted antiferromagnet exhibiting an interesting magnetic orientational phase transition. The crystal structure of the compound is orthorhombic,^{4,5} and its magnetic structure is well known.^{6,7} Although the actual magnetic structure is complicated, for our purposes it can be viewed as a canted two-sublattice antiferromagnet^{8,9} described by magnetic vector \mathbf{M} and antiferromagnetic vector \mathbf{G} . The phase transition happens at $T_{pt} \approx 415$ K between the $\Gamma_2(M_x, G_z)$ and $\Gamma_4(M_z, G_x)$ phases. This transition is in many ways similar to the transitions observed in the widely studied case of orthoferrites, but at the same time shows very distinct characteristics.

Similar to the case of orthoferrites, in the high temperature phase, i.e., below the Neel temperature down to the phase transition temperature, the spins are aligned parallel to the $[100]$ direction and the spontaneous moment is in the $[001]$ direction. This state is labeled Γ_4 ($\mathbf{M} \parallel \mathbf{c} \parallel \mathbf{z} \parallel [001]$). For $T < T_{pt}$ the spins are aligned parallel to the $[001]$ direction and the spontaneous moment is in the $[100]$ direction. That state is labeled Γ_2 ($\mathbf{M} \parallel \mathbf{a} \parallel \mathbf{x} \parallel [100]$). At the transition the weak magnetic moment of the material rotates by 90 degrees in the (\mathbf{a}, \mathbf{c}) crystallographic plane from \mathbf{c} axis to \mathbf{a} axis. It is supposed that, similar to orthoferrites, the reorientation results from temperature variation of the magnetic anisotropy, which passes through zero near the reorientation temperature.⁶

However, there is also a considerable difference. In orthoferrites two subsequent second-order transitions are separated by ~ 10 K temperature interval and can be easily resolved. In the interval between them the magnetization vector \mathbf{M} continuously rotates (see, for example, Refs. 10 and 11). In contrast to that, the reorientation in Fe_3BO_6 is quite abrupt,⁶ with magnetization jumping from one direction to another at the transition point. In the literature it was considered to be the first order transition. For example, in

Ref. 12 a coexistence of the Γ_2 and Γ_4 magnetic phases was observed in a narrow (0.25 K) temperature interval near T_{pt} in a Mössbauer experiment, and a conclusion was drawn about the first-order nature of this reorientation transition. Ultrasound experiments showing anomalous attenuation near the transition point¹³ were also interpreted in terms of the presence of an intermediate state of coexisting Γ_2 and Γ_4 domains.

In the present work the transition was studied by magnetic measurements with the goal of elucidating the nature of the reorientation. Magnetization and coercivity of the Fe_3BO_6 were measured in the broad 4–550 K temperature interval that includes the transition point. The radio-frequency and static susceptibilities were measured near the phase transition temperature. Although the accuracy of our experiment does not allow one to resolve the internal structure of the reorientation transition, the results point to the case of two second-order transitions in close proximity to one another or a weak first-order transition with a small energy barrier between the Γ_2 and Γ_4 phases.

II. EXPERIMENTAL RESULTS

All measurements were performed on the samples of Fe_3BO_6 made of single crystals grown by the flux melting technique.

A. Magnetization and coercivity

Magnetization measurements in the high temperature interval $T=300$ – 600 K were performed on an Oxford Instruments VSM magnetometer. The sample was mounted in a ceramic holder by the Autostic high performance ceramic industrial cement FC8. An automatic rotating magnetometer head allowed for precise alignment of the magnetic axes with the applied field, increasing the accuracy of the measurement. The magnetic moment and coercive force were determined from the hysteresis loops which were typically square-shaped (see Fig. 1). Measurements were performed independently in the Γ_2 and Γ_4 phases.

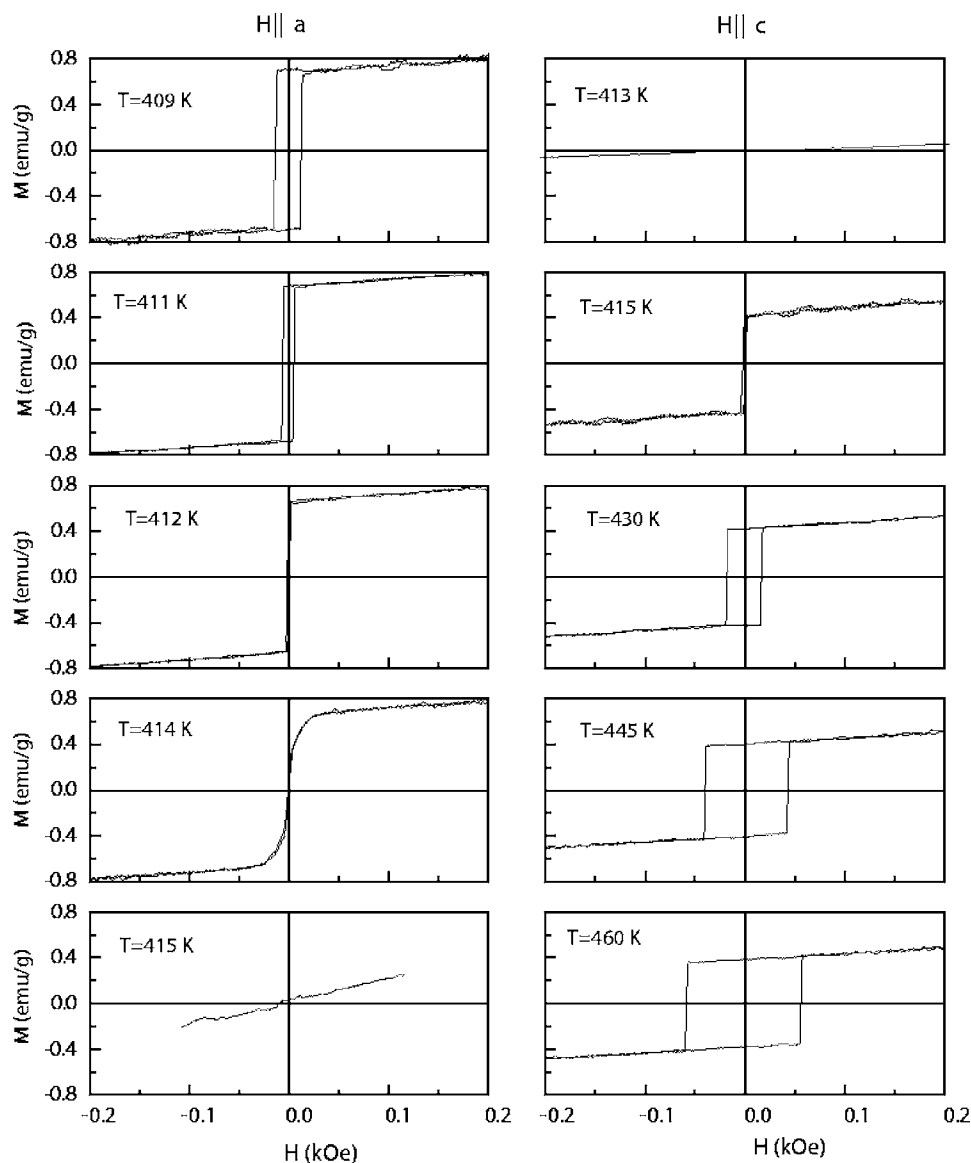


FIG. 1. Magnetization loops $M(H)$ for symmetric directions of the external field.

A note on the temperature measurement protocol. All high-temperature measurements were performed while the temperature was increasing. Due to technical limitations of the apparatus the temperature sensor could not be placed closer than 20 cm from the sample. As a result, the actual temperature of the sample T differed from the measured value \tilde{T} by a nonlinear correction function. The actual temperature was recovered from a polynomial interpolating function $T = \tilde{T} + \Delta T(\tilde{T})$ based on the experimentally observed ΔT at three well-defined reference points: the room temperature T_R , the phase transition temperature T_{pt} , and the Neel temperature $T_N = 508$ K. The method used to determine T_{pt} in our sample is described in the Appendix. This procedure was consistently followed in all measurements and our results are shown as a function of the actual temperature T .

In the low temperature interval $T = 4.2 - 300$ K magnetic properties of the material were studied using a superconducting quantum interference device (SQUID) magnetometer, Quantum Design MPMS-5S. As before, the coercivity and magnetic moment were determined from the hysteresis loops

which typically had a square shape. This property of the loops allows for a simplification of the magnetization measurements: it is enough to measure M in a weak external magnetic field $H \sim 50 - 100$ Oe, as described in Ref. 14. This method substantially decreases the time required to perform the measurements with very small deviation from the more precise approach of loop analysis (see Fig. 2).

The 4.3–300 K and 300–600 K curves were measured in separate experimental setups. Although the temperature measurements were very accurate in the low-temperature interval, the alignment of the magnetic field had an error of about 3 degrees. Due to this uncertainty, and due to the lower accuracy of temperature measurement in the 300–600 K interval, the data from two intervals did not connect perfectly and an extra coefficient was introduced to match the low and high temperature results at $T = T_R$.

The overall results of the magnetization measurement in the 4.2–550 K interval are shown in Fig. 2. They are more accurate than the earlier measurements,^{6,15} but agree with them qualitatively. The 1.5 fold jump of magnetization near T_{pt} reflects the Dzialoshinski exchange anisotropy.¹⁶ This

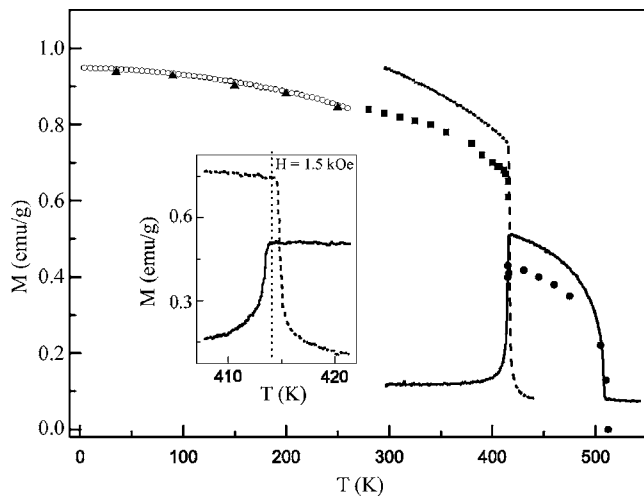


FIG. 2. $M_{a,c}(T)$ extracted from the magnetization loops $M(H)$ for symmetric directions of the external field: filled circles— $(\mathbf{H}\parallel\mathbf{c})$, filled squares— $(\mathbf{H}\parallel\mathbf{a})$, high temperature measurements; filled triangles— $(\mathbf{H}\parallel\mathbf{a})$, low temperature measurements. Empty circles— $M_{a,c}(T)$ measured in a temperature sweep at $H=100$ Oe, $(\mathbf{H}\parallel\mathbf{a})$, low temperature measurements. Dashed line $(\mathbf{H}\parallel\mathbf{a})$ and solid line— $(\mathbf{H}\parallel\mathbf{c})$ —high temperature measurements of $M_{a,c}(T)$ in a temperature sweep at $H=1.5$ kOe. Inset: vicinity of the phase transition at $H=1.5$ kOe. The line corresponds to the phase transition.

mechanism is different from the one operating in orthoferrites,^{14,17–19} where the change of magnetization is driven by the anisotropy of the rare earth susceptibility.

According to our measurement, the abrupt disappearance of the magnetization in one direction and appearance of magnetization in another direction at the transition point happens in a very narrow interval not exceeding 0.5 K (Fig. 2). Only inside of this interval one observes an S-shaped hysteresis loop characteristic of the presence of a domain structure in the sample (Fig. 1, $\mathbf{H}\parallel\mathbf{a}$, $T=414$ K).

If the magnetization is measured in an external field $H=1.5$ kOe, the phase transition temperature slightly shifts as observed in Ref. 6 and as expected from the phase diagram.²⁰ At the same time in the presence of the external field the phase transition broadens to about 2 K and a continuous smooth change of magnetization is observed in this interval. In this case the temperature dependence of magnetization resembles the results obtained for the second order orientation transitions in orthoferrites (see inset in Fig. 2).^{14,17–19}

Figure 3 shows the measured coercive force in the full range of temperatures. Coercive force vanishes near T_{pt} and T_N . Its temperature dependence qualitatively resembles the one followed by the anisotropy field in a field-induced transition from a canted weak ferromagnet state to a spin-flop state.²⁰ The vanishing of the coercive field at T_{pt} is consistent with a very small value of the energy barrier separating two magnetic configurations at the transition point.

B. Radio-frequency susceptibility

Magnetic radio-frequency susceptibility $\chi(T)$ was measured with an autodyne generator (base frequency 6.4 MHz) in a setup analogous to the NMR spectrometer. The reso-

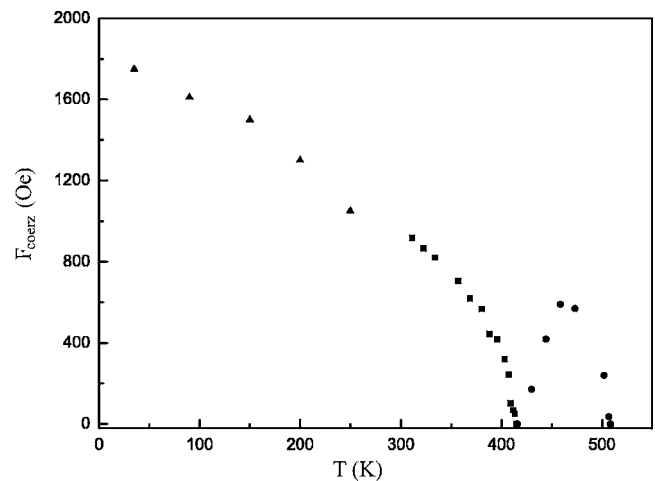


FIG. 3. The coercive field in Fe_3BO_6 extracted from the magnetization loops $M(H)$ for symmetric directions of the external field: circles— $(\mathbf{H}\parallel\mathbf{c})$, squares— $(\mathbf{H}\parallel\mathbf{a})$, high temperature measurements; triangles— $(\mathbf{H}\parallel\mathbf{a})$, low temperature measurements.

nance frequency f of the generator is related to the susceptibility of the sample as $f \sim 1/\sqrt{1+4\pi\chi}$, and was measured with a 10^{-8} relative error. Experiments were performed on a sample in the shape of a slab with dimensions $6.4 \times 3.1 \times 1.02$ mm and with normal vector \mathbf{n} pointing along the crystal axis \mathbf{a} . The sample was placed in a flat rectangular spiral coil coupled to the autodyne generator so that the radio-frequency magnetic field of the coil \mathbf{h} was pointing along the \mathbf{c} crystal axis, $\mathbf{h}\parallel\mathbf{c}$, and the $\chi_c(T)$ susceptibility was measured.

The results are shown in Fig. 4. There was no difference between the up and down sweeps of the temperature. Mea-

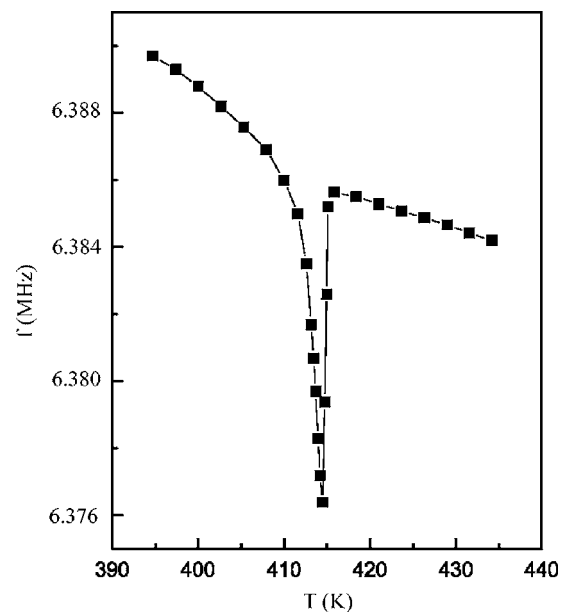


FIG. 4. Temperature dependence of the autodyne generator frequency shift. Anomaly of $f \sim 1/\sqrt{1+4\pi\chi}$ reflects the anomaly of magnetic susceptibility χ and marks the orientation phase transition point.

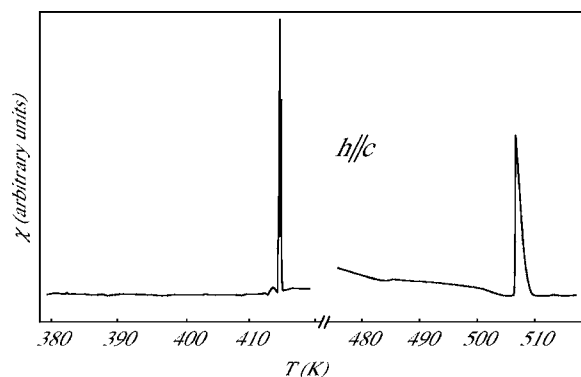


FIG. 5. Temperature dependence of $\chi_c(T)$ near T_N and near T_{pt} for a monodomain sample.

sured $\chi_c(T)$ dependence can be interpreted as follows. When T_{pt} is approached from below, the material is in the $\mathbf{M}\parallel\mathbf{a}$ phase and the radio-frequency magnetic field is perpendicular to the magnetization, thus a nonzero susceptibility is measured. At $T > T_{pt}$ the radio-frequency magnetic field is pointed along the magnetization $\mathbf{h}\parallel\mathbf{c}\parallel\mathbf{M}$ and measures the longitudinal susceptibility, which is expected to be close to zero in a saturated state.

At $T < T_{pt}$ the susceptibility grows below the transition point. This behavior can be explained by the softening of the energy minimum corresponding to the $\mathbf{M}\parallel\mathbf{a}$ phase as the transition is approached. Such interpretation points to the second-order nature of the reorientation transition although it can also be consistent with a weak first-order transition.

C. Static susceptibility

We have also measured the low-frequency magnetic susceptibility of the Fe_3BO_6 crystal. Susceptibility was measured by an autodyne generator with the base frequency of ~ 5.0 MHz in the presence of a modulating magnetic field with an amplitude $h=10$ Oe and frequency $f_m=330$ Hz. The amplitude of the modulating field was chosen to be much larger than the amplitude of the autodyne high-frequency field and thus determined the magnetic state of the sample. The modulation frequency was much smaller than any characteristic frequencies of the system and the resulting susceptibility is equal to the static one. The inductive element of the autodyne was a flat spiral coil. The sample was positioned on top of the coil. The amplitude A of the autodyne signal is detected at the modulation frequency and measures the susceptibility $\chi \sim A$. The temperature dependence $A(T) \sim \chi(T)$ was recorded.

The results are shown in Figs. 5 and 6. When the sample is initially in a monodomain state (e.g., placed into a small constant field ~ 50 Oe which magnetizes the sample and is switched off subsequently), the susceptibility shows a sharp singularity similar to the one observed in the second-order orientation transitions. The $(\mathbf{h}\parallel\mathbf{c})$ susceptibility is shown in Fig. 5. This figure also shows the χ_c susceptibility singularity near the Neel temperature. At T_{pt} the $(\mathbf{h}\parallel\mathbf{a})$ susceptibility exhibits a singularity similar to the one of χ_c . However, χ_a does not have a singularity at T_N in accordance with the

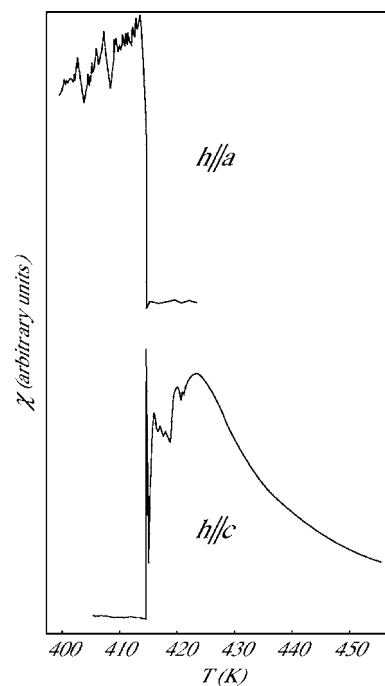


FIG. 6. Temperature dependence of $\chi_a(T)$ and $\chi_c(T)$ near T_{pt} for a multidomain sample.

magnetic anisotropy of the material. Within our accuracy (± 0.2 K) no hysteresis was observed in these measurements.

When the sample is initially in a multidomain state, the phase transition in both $(\mathbf{h}\parallel\mathbf{a})$ and $(\mathbf{h}\parallel\mathbf{c})$ polarizations is manifested as a step (see Fig. 6). The susceptibility is zero on one side of T_{pt} and has an irregular shape on the other side. Sometimes a singularity at T_{pt} is also present (Fig. 6, $\mathbf{h}\parallel\mathbf{c}$). No hysteresis of the step position was observed within our experimental accuracy. The presence of the susceptibility step may be interpreted as the indication of the first-order nature of the transition. However, such a conclusion is not unique, since the same form of $\chi(T)$ can be explained by the presence of the oppositely magnetized domains of the same phase, e.g., Γ_4 for $T > T_{pt}$. In the field $\mathbf{h}\parallel\mathbf{M}$ the domain walls move to increase the size of the domains parallel and decrease the size of those antiparallel to the field and thus produce a nonzero longitudinal susceptibility. This extra susceptibility due to domain wall motion can produce the steps observed in Fig. 6. If the latter explanation is correct, the presence of the same phase domains simply masks the second-order nature of the transition. Due to the finite mobility of the walls such a mechanism is ineffective at higher frequencies which explains why no steps were observed in the 6.4 MHz measurement (Fig. 4).

III. SUMMARY

The Γ_2 - Γ_4 phase transition in Fe_3BO_6 at $T_{pt} \approx 415$ K is characterized by an anomalously narrow spin reorientation interval. In the present work we study several magnetic properties of the material in the vicinity of that transition. Ideally, experiments of this type aim at either resolving the inner structure of the reorientation and identifying it as a sequence

of two second-order transitions, or finding a hysteresis associated with a first-order transition. Although the accuracy of temperature control in the present experiment does not allow for such a direct observation, the behavior is consistent with a transition of a second-, rather than first-order type. Namely, we find a vanishing coercive force and a diverging magnetic susceptibility at the transition temperature.

At the same time, the presence of the mixed state,¹² the jump of the antiferromagnetic resonance frequency,⁹ the lowering of the ultrasound absorption related to the mixed state,^{13,21}—all point to the first-order nature of the transition.

The results of all experiments can be reconciled if one assumes that the phase transition in Fe_3BO_6 is very close to an intermediate transition type, a degenerate case of a transition characterized by a zero energy barrier between two different states. Depending on the manner in which the transition in Fe_3BO_6 crystals deviates from this ideal intermediate case, it should be viewed as either a weak first-order transition with very small hysteresis, or as two second-order phase transitions in close proximity to one another. This situation calls for more theoretical work to understand whether the intermediate nature of the transition in Fe_3BO_6 is accidental or stems from a deeper physical reason.

ACKNOWLEDGMENT

This work was partially supported by the State Fund for Fundamental Research of Ukraine, Project No. F7/203-2004.

APPENDIX: ACCURATE DETERMINATION OF T_{pt} IN A MICROWAVE MEASUREMENT

In the literature, the phase transition temperature of Fe_3BO_6 is quoted as $T_{pt}=415$ K, but should certainly vary somewhat in real crystals. In the present work, transition temperature was carefully determined in a resonance experiment. It is well known (see, for example, Ref. 22), that near the phase transition in Fe_3BO_6 a softening of the iron ions ferromagnetic resonance frequency occurs. This results in resonance absorption of microwave power from a fixed frequency source at two temperature points which are almost symmetric relative to the temperature of the transition. There is also a feature observed right at the transition point.

The microwave measurements were carried out on a direct-gain spectrometer in the regime of reflected power. The sample was glued by its \mathbf{ac} plane in the center of the piston that short circuited the rectangular H_{10} microwave type waveguide. The optimal mutual orientation of the ferromagnetic vector \mathbf{M} and the microwave magnetic field \mathbf{h} for the detection of the soft ferromagnetic mode is $\mathbf{M} \perp \mathbf{h}$. However, to be able to carry out measurements in both the Γ_2 and Γ_4 phases without changing the geometry of the experiment and without remounting the sample, vector \mathbf{h} was oriented at an angle of 45 degrees to the crystal axes \mathbf{a} and \mathbf{c} . The temperature was measured by a thermal emf of a copper-constantan pair.

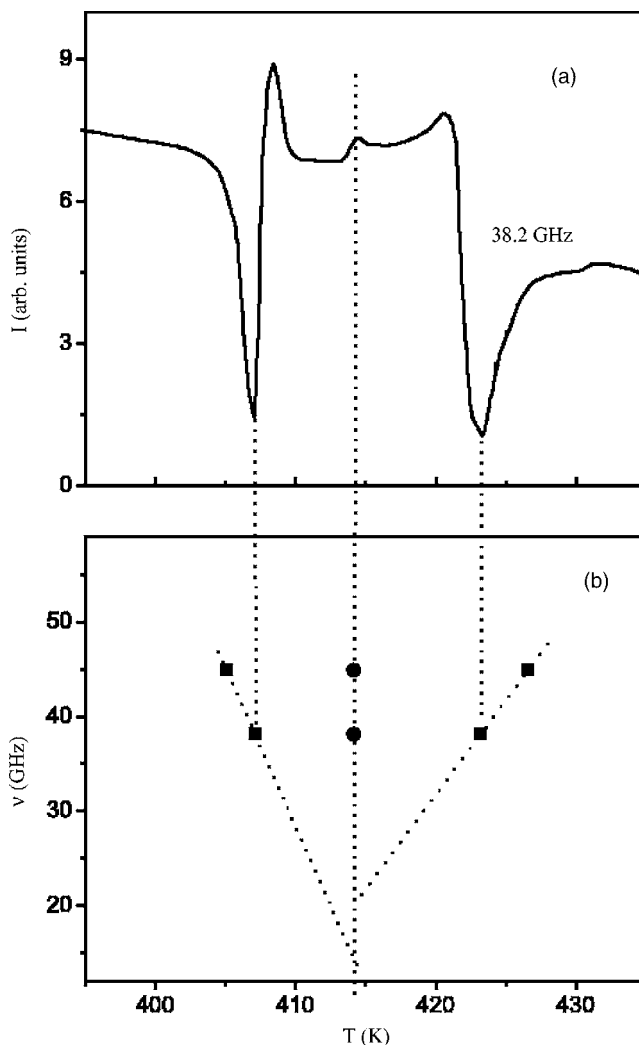


FIG. 7. (a) Plots of the resonance line shape at 38.2 GHz in the vicinity of the spontaneous transition. (b) Resonance points positions at different microwave frequencies.

The result of such measurement at the frequency $\nu = 38.2$ GHz is presented in Fig. 7(a). Figure 7(b) shows the positions of the resonance peaks and the center feature for two frequencies. It is seen that the resonance points move, but the center feature remains at the same temperature point. This way T_{pt} can be reliably extracted from the absorption data. Resonance measurements showed that in our sample the phase transition temperature was equal to $T_{pt} = 414, 1 \pm 0, 1$ K. The measured value of T_{pt} was used as one of the reference points in the high-temperature magnetic measurements performed on the Oxford Instruments vibrating sample magnetometer.

Note that the extrapolated positions of the resonance lines $T_{res}(\nu)$ do not cross exactly at the transition temperature determined by the center feature as already observed in Ref. 22. As a rule such a difference of the gaps is a characteristic feature of the two double second-order Γ_2 - Γ_{24} - Γ_4 transitions.¹¹

*Electronic address: tsymbal@sova.fti.ac.donetsk.ua

- ¹A. V. Kimel, A. Kirilyuk, A. Tsvetkov, R. V. Pisarev, and Th. Rasing, *Nature (London)* **429**, 850 (2004).
- ²N. P. Duong, T. Satoh, and M. Fiebig, *Phys. Rev. Lett.* **93**, 117402 (2004).
- ³A. V. Kimel, A. Kirilyuk, P. A. Usachev, R. V. Pisarev, A. M. Balbashov, and Th. Rasing, *Nature (London)* **435**, 655 (2005).
- ⁴R. Wolfe, R. D. Pierce, M. Eibschutz, and J. W. Nielsen, *Solid State Commun.* **7**, 949 (1969).
- ⁵J. G. White, A. Miller, and R. E. Nielsen, *Acta Crystallogr.* **19**, 1060 (1965).
- ⁶R. Diehl and G. Brandt, *Acta Crystallogr., Sect. B: Struct. Crystallogr. Cryst. Chem.* **B31**, 1662 (1975).
- ⁷V. I. Maltsev, E. P. Naiden, S. M. Zhiliakov, R. P. Smolin, and L. M. Borysyuk, *Kristallografiya* **21**, 113 (1976) (in Russian).
- ⁸E. I. Golovenchits and V. A. Sanina, *Fiz. Tverd. Tela (Leningrad)* **19**, 480 (1977).
- ⁹V. E. Harutunian, K. N. Kocharian, R. M. Martirosian *et al.*, *Int. J. Infrared Millim. Waves* **10**, 841 (1989) [*Zh. Eksp. Teor. Fiz.* **96**, 1381 (1989)].
- ¹⁰R. L. White, *J. Appl. Phys.* **40**, 1061 (1969).
- ¹¹V. D. Buchel'nikov, N. K. Dan'shin, L. T. Tsymbal, and V. G. Shavrov, *Usp. Fiz. Nauk* **166**, 585 (1996) [*Phys. Usp.* **39**, 547 (1996)].
- ¹²A. S. Kamzin, V. A. Bokov, and M. K. Chizhov, *Fiz. Tverd. Tela (Leningrad)* **19**, 2795 (1976).
- ¹³V. Buchelnikov, N. Danshin, D. Dolgushin, A. Isotov, V. Shavrov, L. Tsymbal, G. Kakazei, T. Takagi, and P. Wigen, *J. Magn. Magn. Mater.* **272-276**, 2113 (2004); V. D. Buchel'nikov, N. K. Dan'shin, D. M. Dolgushin, A. I. Izotov, V. G. Shavrov, L. T. Tsymbal, and T. Takagi, *Phys. Solid State* **47**, 1886 (2005) [*Fiz. Tverd. Tela (Leningrad)* **47**, 1813 (2005)].
- ¹⁴Ya. B. Bazaliy, L. T. Tsymbal, G. N. Kakazei, A. I. Izotov, and P. E. Wigen, *Phys. Rev. B* **69**, 104429 (2004).
- ¹⁵M. Hirano, T. Okuda, T. Tsushima, S. Umemura, K. Kohn, and S. Nakamura, *Solid State Commun.* **15**, 1129 (1974).
- ¹⁶E. U. Mullerwiebus and K. A. Hempel, *Physica B & C* **86**, 1261 (1977).
- ¹⁷Ya. B. Bazaliy, L. T. Tsymbal, G. N. Kakazei, and P. E. Wigen, *J. Appl. Phys.* **95**, 6622 (2004).
- ¹⁸L. T. Tsymbal, Ya. B. Bazaliy, G. N. Kakazei, Yu. I. Nepochatykh, and P. E. Wigen, *Fiz. Nizk. Temp.* **31**, 367 (2005) [*Low Temp. Phys.* **31**, 277 (2005)].
- ¹⁹Ya. B. Bazaliy, L. T. Tsymbal, G. N. Kakazei, V. I. Kamenev, and P. E. Wigen, *Phys. Rev. B* **72**, 174403 (2005).
- ²⁰C. Voigt, *Phys. Lett.* **53A**, 223 (1975).
- ²¹L. T. Tsymbal, A. I. Izotov, N. K. Danshin, and K. N. Kocharyan, *Zh. Eksp. Teor. Fiz.* **105**, 948 (1994) [*JETP* **78**, 508 (1994)].
- ²²V. D. Buchel'nikov, N. K. Dan'shin, L. T. Tsymbal, and V. G. Shavrov, *Usp. Fiz. Nauk* **169**, 1049 (1999) [*Phys. Usp.* **42**, 957 (1999)].